



Research paper

Optimization of EphA2 antagonists based on a lithocholic acid core led to the identification of UniPR505, a new 3 α -carbamoxy derivative with antiangiogenic properties

Matteo Incerti ^{a,1}, Simonetta Russo ^{a,1}, Miriam Corrado ^a, Carmine Giorgio ^a,
 Vigilio Ballabeni ^a, Paola Chioldelli ^b, Marco Rusnati ^b, Laura Scalvini ^a,
 Donatella Callegari ^a, Riccardo Castelli ^a, Federica Vacondio ^a, Francesca Ferlenghi ^a,
 Massimiliano Tognolini ^{a,**}, Alessio Lodola ^{a,*}

^a Department of Food and Drug, University of Parma, 43124, Parma, Italy

^b Department of Molecular and Translational Medicine, University of Brescia, 25123, Brescia, Italy

ARTICLE INFO

Article history:

Received 29 July 2019

Received in revised form

16 January 2020

Accepted 19 January 2020

Available online 22 January 2020

Keywords:

EphA2

Lithocholic acid

Protein-protein interaction

SAR

Molecular modelling

Angiogenesis

ABSTRACT

The EphA2 receptor has been validated in animal models as new target for treating tumors depending on angiogenesis and vasculogenic mimicry. In the present work, we extended our current knowledge on structure-activity relationship (SAR) data of two related classes of antagonists of the EphA2 receptor, namely 5 β -cholan-24-oic acids and 5 β -cholan-24-oyl L- β -homotryptophan conjugates, with the aim to develop new antiangiogenic compounds able to efficiently prevent the formation of blood vessels. As a result of our exploration, we identified UniPR505, *N*-[3 α -(Ethylcarbamoxy)oxy-5 β -cholan-24-oyl]-L- β -homo-tryptophan (compound **14**), as a submicromolar antagonist of the EphA2 receptor capable to block EphA2 phosphorylation and to inhibit neovascularization in a chorioallantoic membrane (CAM) assay.

© 2020 Elsevier Masson SAS. All rights reserved.

1. Introduction

The EphA2 receptor is a member of the Eph receptor superfamily of receptor tyrosine kinases [1] whose biological activity is mainly controlled by the ephrin-A1 membrane protein [2]. The EphA2 receptor is overexpressed in a large number of cancers, including brain, prostate, breast, colon, pancreatic and lung cancers [3,4]. Compelling evidences demonstrate that its uncontrolled activation concurs to cancer progression [5] by sustaining an efficient self-renewal of tumor-propagating cells [6], the acquisition of

a migratory phenotype, and the formation of new blood vessels by angiogenesis [7] and vasculogenic mimicry [8,9]. In this scenario, the EphA2 receptor has emerged as a promising target for the development of new, alternative antiangiogenic therapies [10,11]. Three key strategies can be used to inhibit the tumorigenic activity of the EphA2 receptor. The first is based on ATP-mimicking agents targeting the intracellular kinase domain of Eph receptor [12,13]. The second targets the SAM domain of EphA2 [14,15], an intracellular region of the receptor endowed with a regulatory role on its kinase activity [16]. The third relies on molecular agents targeting the extracellular ligand-binding domain (LBD) of EphA2 [17,18], thus preventing its direct interaction with ephrin-A1 [19,20].

Regarding the first approach, kinase inhibitors targeting Eph receptors were initially synthesized starting from the benzamide scaffold of nilotinib (Chart 1). This approach led to the dual EphB4/VEGFR inhibitor NVP-BHG712 [10] and the two multi-kinase inhibitors (ALW-II class) developed by the Gray group at the Harvard Medical School in Boston [21]. While not specifically selective for the Eph kinases, these compounds were used to corroborate the

Abbreviations: PPI, protein-protein interaction; EphA2, ephrin receptor A2; LCA, lithocholic acid; ELISA, enzyme-linked immunosorbent assay; CAM, chorioallantoic membrane.

* Corresponding author.

** Corresponding author.

E-mail addresses: massimiliano.tognolini@unipr.it (M. Tognolini), alessio.lodola@unipr.it (A. Lodola).

¹ These authors contributed equally to this work.

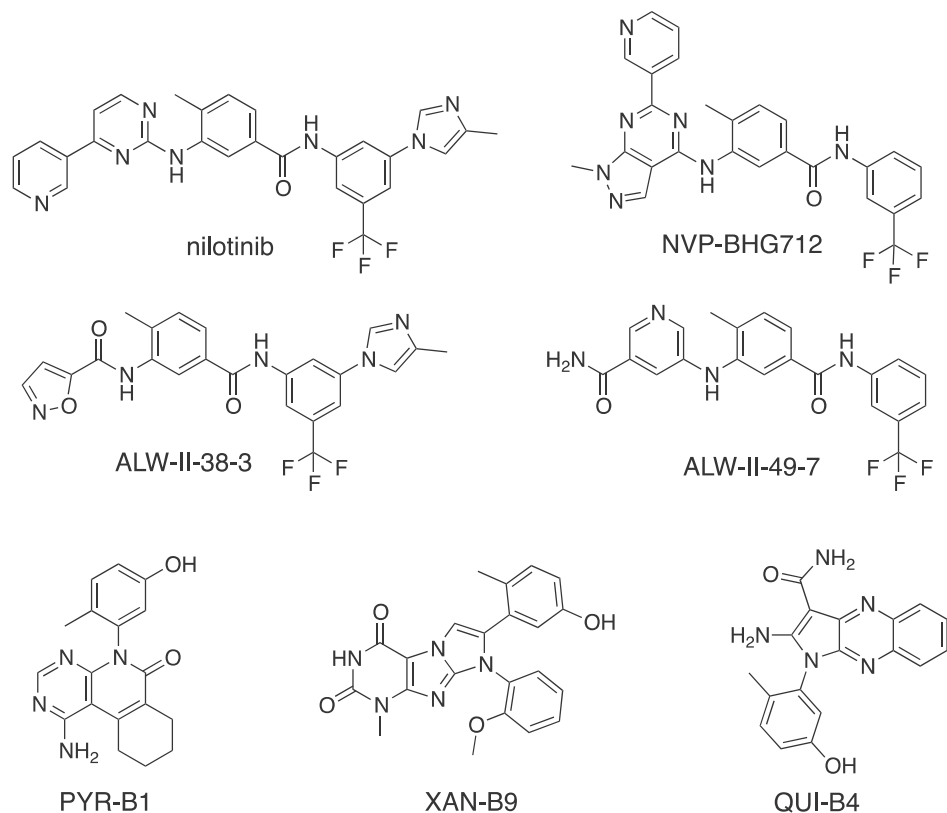


Chart 1. Relevant kinase inhibitors targeting the intracellular kinase domain of Eph receptors.

role played by the Eph-ephrin system in angiogenesis and in insulin homeostasis. A second generation of Eph kinase inhibitors was developed by Caflisch and Nevado at the University of Zurich. This includes three distinct classes of compounds exemplified by *i.* the pyrimidoisoquinolinone PYR-B1 [22], *ii.* the xanthine XAN-B9 [23], and *iii.* the pyrrolo[3,2-*b*]quinoxaline QUI-B4 [24]. These inhibitors displayed nanomolar activity on EphB4 and were also featured by a fair degree of selectivity, according to a kinome scan assay.

While the development of agent targeting the SAM domain is still in its infancy with only few active peptides being available [25], the disruption of Eph-ephrin interaction is reaching a maturity stage with several peptidomimetics [26] and small molecules reported in the literature [27]. Within the pool of small molecules targeting EphA2 LBD [28], bile acid conjugates and related derivatives have emerged as promising EphA2 antagonists useful for treating highly vascularized tumors (Chart 2) [29]. Besides lithocholic acid (LCA, 5 β -cholan-24-oic acid **1**), a weak competitive inhibitor of the EphA2-ephrin-A1 association [30], its *L*- β -homo-tryptophan conjugate, known as UniPR129 (*N*-(3 α -hydroxy-5 β -cholan-24-oyl)-*L*- β -homotryptophan, **2**) was identified as a potent inhibitor of this protein-protein interaction [31,32]. The use of compounds **1** and **2** as pharmacological tools has been limited by their suboptimal pharmacodynamic and pharmacokinetic properties [33]. Our recent investigations demonstrated that the replacement of the 3 α -hydroxyl group with the 3 α -carbamoyloxy one on the nucleus of compound **2** led to inhibitors featuring better pharmacodynamics or pharmacokinetics properties. However, the success of this exploration was only partial as compound **12** (UniPR502), displayed cytotoxic effects on HUVEC cells at high doses [34]. Here, we tried to exploit the aforementioned carbamoyloxy functionality to introduce a point for chemical diversification into the 5 β -cholan-24-oic acid scaffold, to design better Eph-ephrin antagonist. We report the result of our SAR investigation

around 3 α -carbamoyloxy-5 β -cholan-24-oic acid (A-series) and *N*-(3 α -carbamoyloxy-5 β -cholan-24-oyl)-*L*- β -homo-tryptophan conjugate (B-series) by modification of the substituent at the nitrogen atom of 3 α -carbamoyloxy group in the search for new EphA2 antagonists.

2. Chemistry

Lithocholic acid (LCA, **1**) was purchased from Sigma (Milano, Italy) while compounds **3** and **12** were synthesized according to the procedure described in Refs. [31,35]. The 3 β -carbamoyloxy-5 β -cholan-24-oic acid **4** and its corresponding *L*- β -homo-tryptophan conjugate **13** were synthesized following the steps reported in Scheme 1. The inversion of configuration of the 3 α -hydroxyl group of LCA resulted from the Mitsunobu reaction between LCA methyl ester **4e** and acetic acid. The obtained 3 β -acetyl derivative was then hydrolyzed to give compound **4c**. The 3 β -carbamoyloxy-5 β -cholan-24-oic acid **4** was synthesized reacting the methyl ester **4d** with potassium isocyanate, and the following hydrolysis of the ester group with NaOH. The *N*-(3 β -carbamoyloxy-5 β -cholan-24-oyl)-*L*- β -homo-tryptophan **13** was obtained by conjugation of compound **4** with the *L*- β -homo-tryptophan methyl ester hydrochloride, using *N*-(3-dimethylaminopropyl)-*N'*-ethylcarbodiimide hydrochloride (EDCI) as coupling agent. The resulting amide **13a** was then hydrolyzed with NaOH to give the title compound **13**.

Compounds **5–11** and **14–20** were synthesized according to the procedure reported in Scheme 2. The *N*-substituted carbamates at position 3 of LCA **5–11** were obtained reacting the LCA methyl ester **4e** with the corresponding *N*-alkyl/aryl-isocyanate. The obtained methyl ester derivatives **5a–11a** were hydrolyzed to yield compounds **5–11**. These compounds were then coupled with the *L*- β -homo-tryptophan methyl ester hydrochloride following the same procedure described in the Scheme 1, to provide the corresponding

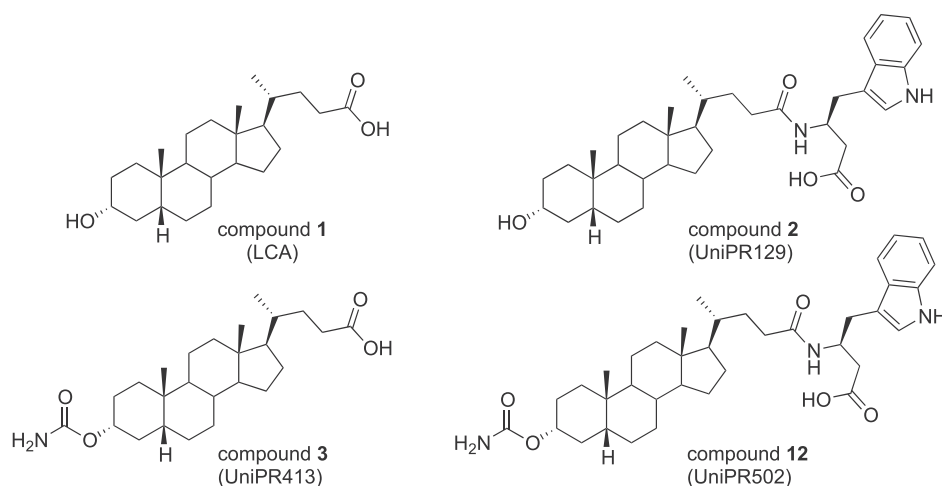
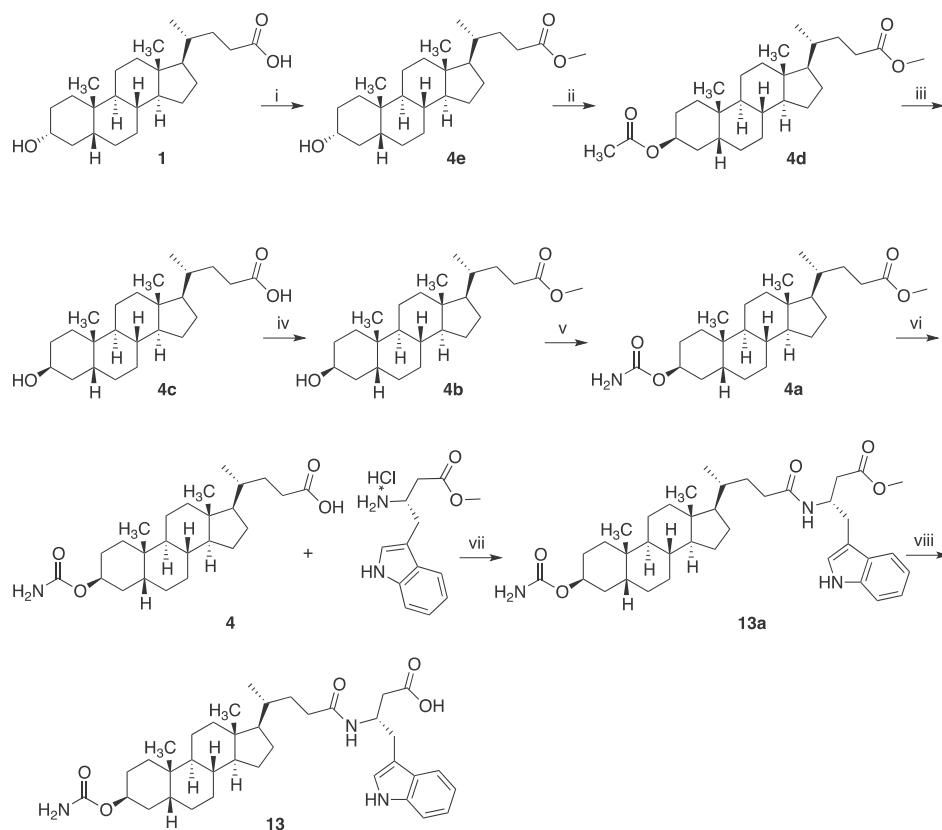


Chart 2. Structures of EphA2 receptor antagonists featured by a the 5β-cholan-24-oic acid scaffold.



Scheme 1. Reagents and conditions: i) H_2SO_4 , CH_3OH , r.t., 4 h; ii) PPh_3 , DIAD, CH_3COOH , THF, 0°C – r.t., overnight; iii) $\text{KOH}_{(\text{aq})}$ 15%, EtOH, reflux, 3 h; iv) H_2SO_4 , CH_3OH , r.t., 4 h; v) NCOK , CF_3COOH , toluene, reflux, overnight; vi) $\text{NaOH}_{(\text{aq})}$ 15%, EtOH, r.t. 1 h; vii) NMM , EDCI , CH_2Cl_2 , r.t., overnight; viii) $\text{NaOH}_{(\text{aq})}$ 15%, EtOH, r.t. 1 h.

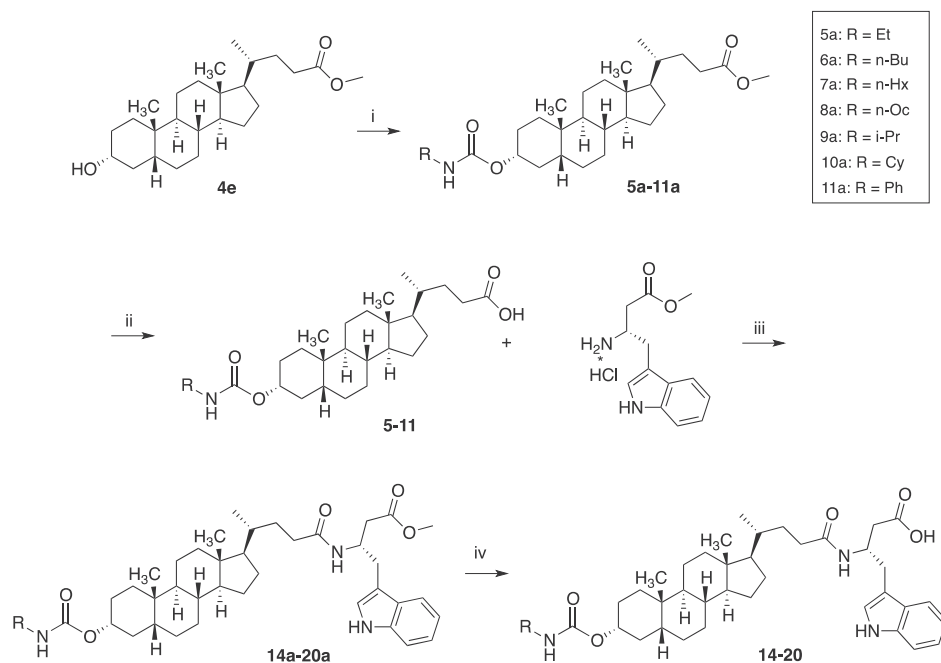
amide conjugates **14a–20a**. The final products **14–20** were obtained by hydrolysis of the methyl ester.

3. Results and discussion

3.1. SAR analysis of 3-carbamoyloxy derivatives of 5β-cholan-24-oic acid and 5β-cholan-24-oyl-L-β-homo-tryptophan conjugates

3α -carbamoyloxy-5β-cholan-24-oic acid **3** [35] and N -(3α -carbamoyloxy-5β-cholan-24-oyl)-L-β-homo-tryptophan conjugate **12**

[36] were used as template structures to develop two focused series of N -primary carbamates that were then evaluated for their ability to prevent ephrin-A1 binding to EphA2 by using a previously validated ELISA binding assay [32]. The IC_{50} values for the reference and newly synthesized compounds are reported in Tables 1 and 2 (A- and B-series, respectively). Previous investigations have shown that compound **3** [35] and **12** [36] likely engage the EphA2 receptor with a different binding mode, i.e. with the free-carboxyl group forming a salt bridge with Arg159 in case of **3** or with Arg103 as for compound **12** (Fig. 1). In line with these findings, a



Scheme 2. Reagents and conditions: i) RNCO, toluene, reflux, overnight; ii) NaOH_(aq) 15%, EtOH, r.t. 1 h; iii) NMM, EDCI, CH₂Cl₂, r.t., overnight; iv) NaOH_(aq) 15%, EtOH, r.t. 1 h.

different profile for the two newly explored series is expected in term of SAR.

As a first step in our exploration, we investigated the role of the absolute configuration of the carbamoyloxy group at position 3 of the steroidal scaffold. We thus synthesized the 3 β -carbamoyloxy derivatives of both free acid derivative and *l*- β -tryptophan conjugate, compound **4** (Table 1) and **13** (Table 2). The inversion of configuration of the stereocenter in position 3 was tolerated in the case of the A-series, while it led to a loss of inhibitory potency in the case of the B-series. Then, we focused our attention on the synthesis of compounds with the α configuration at the position 3 of the steroidal nucleus of both A- and B- series.

We next interrogated the effect on the inhibitory potency of substituents with varying stereoelectronic properties at the nitrogen atom of 3 α -carbamoyloxy group. At first, an ethyl group was

inserted on the nitrogen of the 3 α -carbamoyloxy-5 β -cholan-24-oic acid. The obtained compound **5** showed an IC₅₀ of 30 μ M, slightly higher than that of the reference compound **3** (IC₅₀ = 17 μ M). Further, a remarkable improvement of potency was obtained with the elongation of two carbon units of the ethyl substituent. The *N*-butyl(carbamoyloxy)-derivative **6** resulted indeed more potent than compound **3**, with an IC₅₀ of 3.7 μ M. Similarly, the introduction of a *N*-hexyl substituent provided a compound with a good potency (**7**, IC₅₀ = 3.3 μ M). A further elongation of the linear alkyl chain was still tolerated, as revealed by the IC₅₀ value of the octyl-derivative **8** (IC₅₀ = 4.5 μ M). Introducing a small branched alkyl substituent (isopropyl) resulted in compound **9**, which turned out to be endowed with an IC₅₀ equal to 12 μ M, thus less potent than the linear alkyl chain-derivatives **6**–**8**. The inclusion of the isopropyl group into a cyclohexyl substituent led to compound **10**,

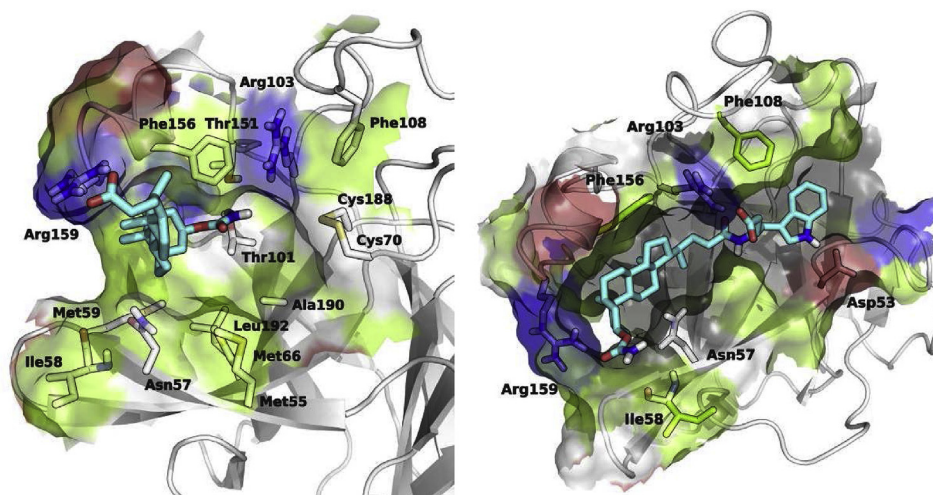
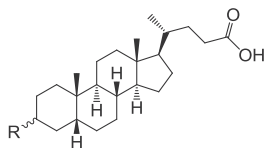


Fig. 1. Binding mode of **3** (left panel) [35] and **12** (right panel) [36] within the LBD domain of the EphA2 [37] deduced by free-energy simulations. EphA2 surface is coloured according to the electrostatic potential (red, negative; blue positive; green neutral), while ligand carbon atoms are represented with cyan tube. (For interpretation of the references to colour in this figure legend, the reader is referred to the Web version of this article.)

Table 1

IC₅₀ values for 3-substituted derivatives of 5β-cholan-24-oic acid 3–11 obtained from EphA2-ephrin-A1 displacement experiments.



Cpd	R-	IC ₅₀ (μM) ^a
1	HO ^{•••}	79 ^b (67–93)
3		17 (8.7–35)
4		9.1 (6.1–14)
5		30 (20–44)
6		3.7 (2.9–4.6)
7		3.3 (2.4–4.5)
8		4.5 (3.2–6.3)
9		12 (8.9–14)
10		2.7 (2.1–3.4)
11		38 (21–68)

^a Values are the mean from at least three independent experiments. Numbers in brackets denote the 95% confidence interval for IC₅₀.

^b Value from Ref. [36].

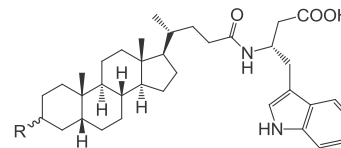
featuring a higher potency (IC₅₀ = 2.7 μM) and supporting the importance of undertaking lipophilic interaction at the EphA2 receptor. However, the replacement of a cyclohexyl substituent with a phenyl one was barely tolerated, as indicated by the low inhibitory potency of **11** (IC₅₀ = 30 μM). It could be devised that, in addition to lipophilicity, a mutual stereoelectronic complementarity between the inhibitor and EphA2 receptor is indeed critical.

Docking of **5–11** within the ligand binding domain of EphA2 (see *Experimental section for details*) reveals that these compounds can assume a pose comparable to that of **3**, i.e. with the carboxylic group interacting with Arg159 and the chain emerging from the carbamic nitrogen atom pointing toward a lipophilic pocket delimited by two cysteines (Cys70 and Cys188) involved in a disulfide bridge (Fig. 2). The most active inhibitors of this series (**7**, **8** and **10**) undertakes several productive contacts within the EphA2 receptors. This is not the case for compound **11** that due to the accommodation assumed by its phenyl ring undertakes several clashes with the protein surface.

The same linear and branched substituents were inserted on the nitrogen of the *N*-(3α-carbamoyloxy-5β-cholan-24-oyl)-L-β-homo-

Table 2

IC₅₀ values for 5β-cholan-24-oyl-L-β-homo-tryptophan derivatives 12–20 measured in EphA2-ephrin-A1 displacement experiments.



Cpd	R-	IC ₅₀ (μM) ^a
2	HO ^{•••}	0.91 (0.80–1.1) ^b
12		1.2 (0.85–1.6)
13		5.2 (3.0–9.1)
14		0.95 (0.60–1.5)
15		1.1 (0.70–1.8)
16		1.5 (1.2–2.0)
17		15 (13–17)
18		7.1 (3.9–13)
19		1.2 (0.94–1.5)
20		5.5

^a Values are the mean from at least three independent experiments. Numbers in brackets denote the 95% confidence interval for IC₅₀.

^b Value from reference [36].

tryptophan conjugate **12**, prototypical member of the B-series. In this case, the substitution with ethyl- and butyl-groups led to highly potent compounds, **14** and **15**, with an IC₅₀ value of 0.95 μM and 1.1 μM, respectively, thus in range with the reference compound **12** (IC₅₀ = 1.2 μM). The elongation of the linear alkyl chain provided by hexyl substituent led to compound **16**, showing a comparable potency (IC₅₀ = 1.5 μM) with respect to the shorten *N*-alkyl substituted-carbamates. The further lengthening of the alkyl chain obtained with the octyl substituent resulted detrimental for binding EphA2 receptor. As demonstrated by compound **17**, that displayed a marked decrease of potency (IC₅₀ = 15 μM), the hydrophobic pocket of EphA2 receptor accounts limited space to host the alkyl-substituent of the carbamate-moiety. The introduction of an iso-propyl group led to a less potent derivative (**18**, IC₅₀ = 7.1 μM) with respect to the reference compound **12**. Analogously, a cycloalkyl-substituent was tolerated better than a free branched alkyl group, as demonstrated by the cyclohexyl-derivative **19** that showed an inhibitory potency (IC₅₀ = 1.0 μM) similar to that of the best compounds of the series. Finally, the

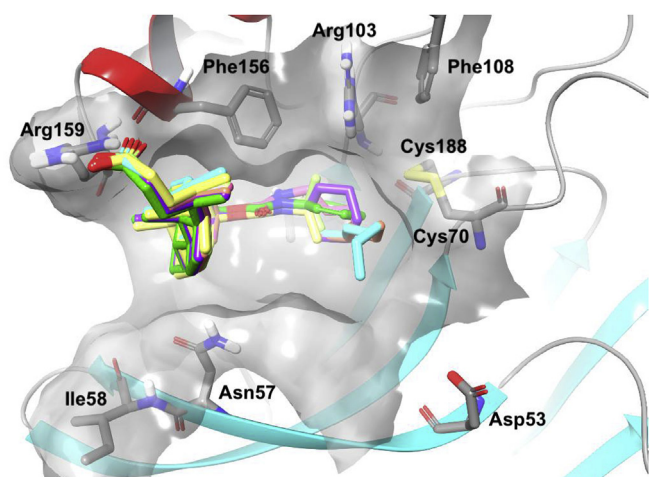


Fig. 2. Docking of compound **5–11** within the LBD domain of the EphA2. EphA2 surface is coloured in white, while ligand carbon atoms are represented with different colours. The most actives are in cyan (compound **8**) and in magenta (compound **10**). (For interpretation of the references to colour in this figure legend, the reader is referred to the Web version of this article.)

replacement of the *N*-cyclohexyl group with a *N*-phenyl one led to compound **20** which had a slightly higher IC_{50} value, indicating that aromatic substituents are tolerated by EphA2 receptor at this position. Overall, this exploration points out that while it is possible to reach single-digit micromolar concentration with 3-substituted 5 β -cholan-24-oic acid derivatives (as for compounds **3**, **6** or **10**), sub-micromolar potency can be reached only with 5 β -cholan-24-oyl- ι - β -homo-tryptophan conjugates (as for compound **14**).

Docking of **14–20** within the LBD of EphA2 shows that these compounds are able to assume the same binding pose of the parent compound **12**, i.e. with the carboxylic group of the ι - β -homo-tryptophan moiety forming a salt bridge with Arg103 and the lipophilic substituent at the carbamic nitrogen atom pointing toward the exit of the EphA2 binding pocket, flanking Ile58 (Fig. 3). Such accommodation accounts for the tolerance of EphA2 with respect to the size and shape of the substituent in position 3 of nearly all the tested ι - β -homo-tryptophan conjugates (i.e. compounds **14–16**, **18–20**) and for the loss of activity displayed by **17**, in light of its long octyl chain which extends beyond the EphA2 pocket reaching the bulk solvent.

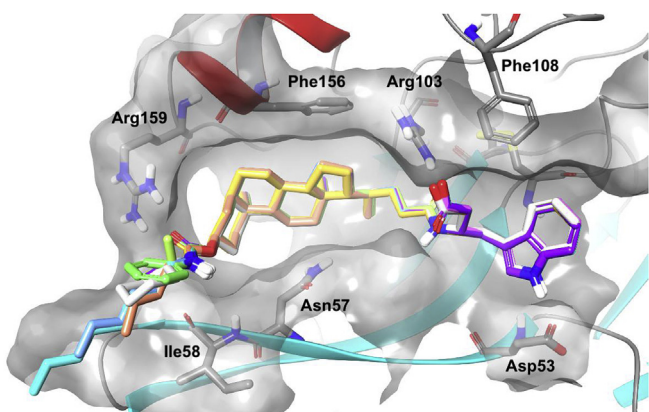


Fig. 3. Docking of compounds **14–20** within the LBD domain of the EphA2. EphA2 surface is coloured in white, while ligand carbon atoms are represented with different colours. The most actives are in magenta (compound **14**) and in orange (compound **15**). (For interpretation of the references to colour in this figure legend, the reader is referred to the Web version of this article.)

The docking poses for compounds **14–20** reinforce the concept that the ι - β -homo-tryptophan moiety is important for the activity, as its aromatic $-NH$ group is involved in a hydrogen bond with Asp53. In agreement with this model, a previously reported SAR study around UniPR129 showed that the replacement of the indole with a thiophen or a naphthyl ring led to a moderate reduction in the inhibitory potency [36]. On the same line, a significant loss in the potency was observed inverting the chirality of the β -carbon bearing the indol-3-ylmethyl chain.

3.2. Activity on EphA2 phosphorylation in human prostate adenocarcinoma (PC3) cells

Among all the synthesized compounds, we focused our attention on those belonging to the B-series which displayed higher inhibitory potency in the displacement assay, and we selected antagonists with an IC_{50} value lower than 5 μ M. These compounds were then tested for their ability to interfere with EphA2 activation in human prostate adenocarcinoma (PC3) cells, which naturally overexpress the EphA2 receptor [38]. PC3 cells were incubated for 20 min with increasing concentration of compounds **12**, **14–16** and **19**, further stimulated for 20 min with ephrin-A1 (0.25 μ g/ml) and then evaluated for EphA2 phosphorylation using an ELISA assay. All the compounds dose-dependently inhibited EphA2 phosphorylation, with **14** emerging as the most potent compound of the series, with an IC_{50} equal to 1.5 μ M, that is very close to the inhibitory activity displayed in the cell-free displacement assay (Fig. 4). All the compounds did not alter EphA2 phosphorylation on their own (data not shown) and did not exert any specific toxic effect on PC3 cells, as assessed by LDH assay after 2h of compound incubation (Fig. S1, supplementary data). Taken together, these results indicate the specificity of the observed reduction in the phospho-EphA2 level, that can be genuinely linked to a direct action of the compounds at the EphA2 receptor.

3.3. Molecular mechanism of action of compound **14** at the EphA2 receptor

Among all the compounds tested in the EphA2 phosphorylation assay, we focused our attention on compound **14** whose mechanism of action was investigated at a molecular level. To this aim, binding curves describing ephrin-A1 association to EphA2 up to saturation were built in the presence of increasing concentrations of compound **14** (Fig. 5). The parallel rightward shift of saturation

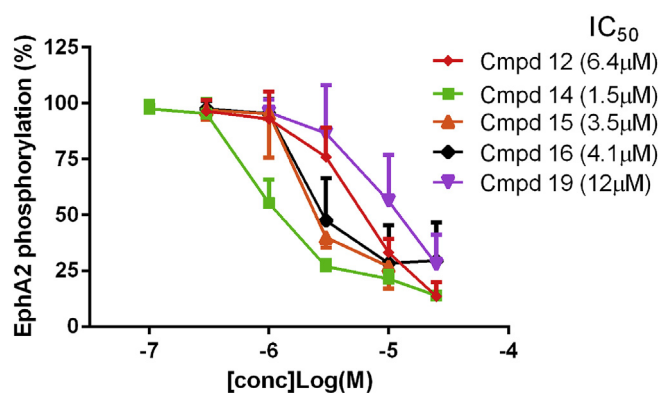


Fig. 4. Concentration-dependent inhibition of ephrin-A1-induced activation of EphA2. Cells were pretreated for 20 min with 0.3% DMSO or with the indicated concentrations of compounds and then stimulated for 20 min with ephrin-A1-Fc 0.25 μ g mL $^{-1}$. Phospho-EphA2 levels are relative to ephrin-A1-Fc + 0.3% DMSO. Data are the means \pm st.dev of at least 3 independent experiments.

dose–response curves with no significant alteration of the maximal response suggests a competitive mechanism of action for compound **14**. Relevant to note, with an inhibitory constant (K_i) equal to 0.3 μM , compound **14** is among the most potent antagonists of the EphA2 receptor reported in the literature, slightly superior to its close analogue **12**, and comparable to the reference antagonist UniPR129 [32], which were reported to have K_i values of 0.8 and 0.4 μM , respectively.

3.4. Selectivity profile of compound **14** on a panel of Eph receptors

Beside EphA2-EphrinA1, other Eph-ephrin signaling axes are involved in physiological and pathological processes, prompting us to evaluate the selectivity of compound **14**. To this aim, its ability to interfere with ephrin binding to EphA1-EphA8 and EphB1-EphB4 receptor subtypes was evaluated in a displacement assay where biotinylated ephrin-A1-Fc and ephrin-B1-Fc were employed as EphA or EphB receptor ligands, respectively. Diverging from previously reported 3 α -hydroxy-5 β -cholan-24-oyl amino acid conjugates (including **12**, able to engage all the Eph receptors with comparable inhibitory potency [34]), compound **14** demonstrated a moderate preference for the EphA2 (Table 3). Further, the lack of activity on some receptors (i.e. EphA1, EphA7, EphB1, EphB4 and EphB6) suggests that the position 3 on the 5 β -cholan-24-oyl core could be exploited for improving receptor selectivity.

3.5. Antiangiogenic properties of compound **14** on chicken egg CAM assay

The EphA2-ephrin-A1 signaling axis has been reported to be critical for angiogenesis [39]. Compounds able to disrupt EphA2-ephrin-A1 interaction are expected to dramatically hamper the formation of blood vessels and are potentially useful for cancer treatment. Fig. 6 shows that compound **14** dose-dependently inhibits the ability of HUVE cells to organize themselves in relatively large vessels in the presence of a polymeric scaffold known as Matrigel [40]. The IC_{50} for this process was close to 3 μM , consistent with the activity observed in both the displacement assay and the phosphorylation test. Again, at the tested concentrations, compound **14** did not display cytotoxic effects on HUVECs when tested with LDH assay after 2 and 16 h of incubation and with MTT after 16 h up to 30 μM (Fig. S2, supplementary data).

In light of these encouraging results, the antiangiogenic properties of compound **14** were investigated in the chick chorioallantoic membrane (CAM), which is a model of *in vivo* neovascularization. In the CAM model, it is possible to follow the formation of primitive vessels and their differentiation to a functional arteriovenous system in the presence of soluble angiogenic

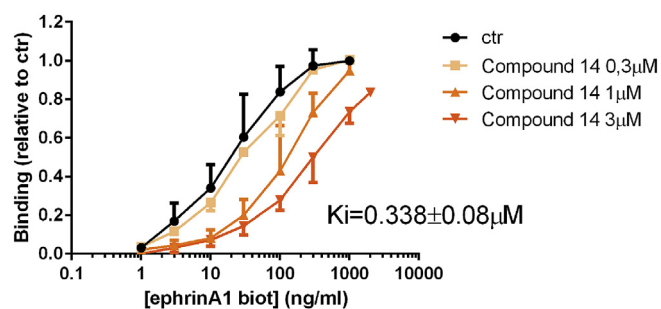


Fig. 5. Saturation curves of biotinylated ephrin-A1-Fc on EphA2 built in presence of increasing concentration of compound **14**. The inhibition constant (K_i) was calculated using Prism non-linear regression analysis. Data are the means \pm st.dev. of three independent experiments.

Table 3

IC_{50} values of compound **14** measured in displacement experiments for EphA1-EphA8 and EphB1-EphB4, EphB6, in the presence of biotinylated ephrin-A1-Fc or ephrin-B1-Fc.

Receptor subtype	IC_{50} (μM) ^a
EphA1	>30
EphA2	0.95 (0.60–1.5)
EphA3	4.5 (2.8–7.1)
EphA4	6.4 (3.1–13)
EphA5	4.4 (2.5–7.9)
EphA6	18 (9.2–36)
EphA7	>30
EphA8	7.7 (4.0–15)
EphB1	>30
EphB2	14 (6.5–29)
EphB3	11 (4.9–25)
EphB4	>30
EphB6	>30

^bNumbers in brackets denote the 95% confidence interval for IC_{50} .
^a Values are the mean from at least three independent experiments.

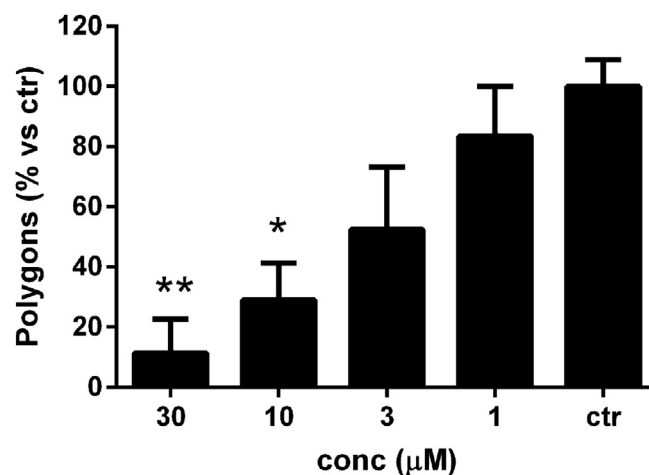


Fig. 6. Angiogenesis assay for compound **14**. The number of polygons measured is relative to PBS solution with 1% DMSO, used as the control. The histogram shows the means of three independent experiments \pm SEM. One-way ANOVA followed by Tukey's post-test was performed to compare the control to all other conditions. * $P < 0.05$, ** $P < 0.01$.

growth factors. It is also possible to evaluate the inhibitory effect of small molecules [41]. As the VEGF/VEGFR and Eph-ephrin systems cooperate in promoting the formation of blood vessels [42,43] we evaluated the effect of compound **14** on VEGF-dependent neovascularization. VEGF alone determined a substantial increase in the number of vessels that was significantly blocked by compound **14** (Fig. 7). On the opposite, compound **14** has no effect on the basal, unstimulated angiogenesis of the CAM, further adding to the specificity of its inhibitory effect (Fig. 7).

Differently to what observed for the EphA2 antagonist **14** (UniPR505), the parent compound **12** (UniPR502) promoted the growth of new vessels when tested alone in the CAM model (Fig. S3, supplementary data). We ascribed this phenotypic response to the low selectivity displayed by UniPR502 in light of its ability to target all the members of the Eph receptor family with comparable potency. In this respect, the higher selectivity displayed by compound **14** (Table 3), with a moderate preference for EphA2, leads to an improved pharmacological profile when this compound is tested on endothelial cells.

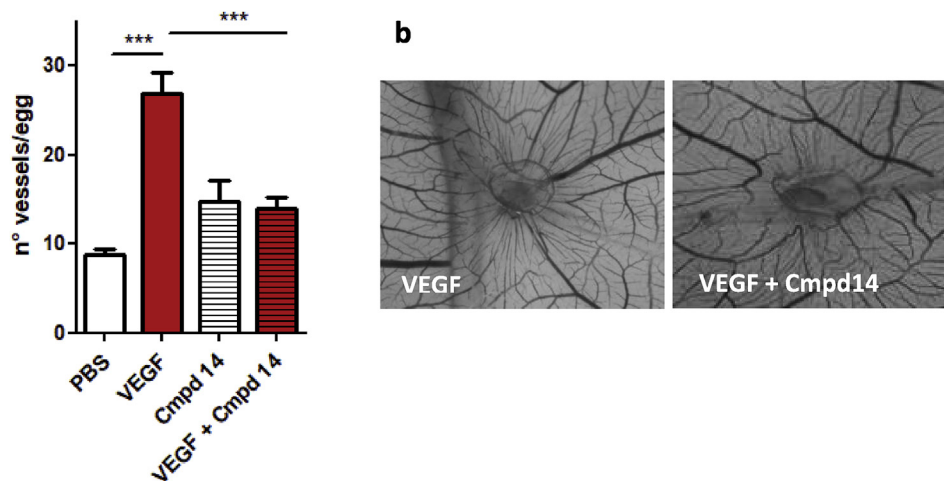


Fig. 7. (a) Number of vessels per egg in presence of VEGF (positive control) or PBS solution (negative control) and/or after adding 10 μM of compound **14**. Data are the mean \pm SEM of 3 independent experiments ***: $p < 0.001$, one-way ANOVA followed by Dunnett's post-hoc test. (b) Representative photographs of CAMs incubated with VEGF and **14**.

4. Conclusions

The EphA2 receptor is a key factor in several cancers where its activity correlates with tumor stage and progression particularly in the case of glioblastoma [29]. Although some promising agents that target the EphA2 receptor kinase domain or that bind and mask its ectodomain have been already described, no drugs acting specifically on this receptor have been approved so far. In the present work, we describe the synthesis and pharmacological characterization of compound **14**, a new EphA2 antagonist with sub-micromolar affinity for the EphA2 LBD domain and able to block ephrin-dependent signals in cancer cells at low micromolar concentration. Consistently with its activity on the Eph-ephrin system, compound **14** markedly blocks the formation of new blood vessels in a CAM assay, in the presence of growth factors. Compared to previously reported EphA2 antagonists featured by a 5β -cholan-24-oyl core [36] or by a Δ^5 -cholen-24-oyl structure [44,45], compound **14** displays higher selectivity for the EphA2 receptor and can be thus considered as one of the most interesting antagonist reported so far, which deserves further investigations in animal models of cancer.

5. Experimental section

5.1. Chemistry

Unless otherwise noted, reagents and solvents were purchased from commercial suppliers and were used without purification. The progress of the reaction was monitored by thin-layer chromatography with F₂₅₄ silica-gel precoated sheets (Merck, Darmstadt, Germany). UV light and a solution of ammonium molybdate and ceric sulfate in aqueous sulfuric acid (5% v/v) were used for detection. Flash chromatography was performed using Merck silica-gel 60 (Si 60, 40–63 μm , 230–400 mesh ASTM). Dichloromethane was dried by distillation over calcium hydride. All reactions were carried out using flame-dried glassware under atmosphere of nitrogen. Melting points were determined on a Gallenkamp melting point apparatus and were not corrected. The ¹H NMR and ¹³C NMR spectra were recorded on a Bruker Avance 400 spectrometer (400 MHz); chemical shifts (δ scale) are reported in parts per million (ppm). ¹H NMR spectra are reported in the following order: multiplicity, approximate coupling constants (*J* value) in Hertz (Hz) and number of protons; signals were

characterized as s (singlet), d (doublet), t (triplet), q (quartet), m (multiplet), bs (broad signal). Mass spectra were recorded on an Applied Biosystem API-150 EX system spectrometer using an ESI interface. Compounds **3–23** were prepared according to the synthetic procedures described in the Supplementary Data. The purity of each compound was assessed by HPLC/MS and elemental analysis (ThermoQuest FlashEA 1112 elemental analyzer for C, H, and N). All tested compounds were >95% pure by HPLC analysis and had acceptable C, H, N analysis results (within ± 0.4 of theoretical values).

5.2. Molecular modelling

Docking studies were performed with Glide [46] using the atomic coordinates of the EphA2 receptor (pdb code: 3HE1 [37]) taken from equilibrated complexes (by plain molecular dynamics simulations) of its ligand binding domain with **1** (LCA, see Ref. [35]) or **2** (UniPR129, see Ref. [36]). Compounds **5–11** were docked in the EphA2 structure equilibrated with **1**, while **14–20** were docked in the EphA2 structure equilibrated with **2**. In both cases, docking grids were centered in the channel of the EphA2 receptor delimited by Arg103, Phe108, Phe156 and Arg159. Dimensions of enclosing and bounding boxes were set to 20 and 10 Å on each side, respectively, and van der Waals radii of protein atoms were not scaled during grid generation. The structures of the docked compounds were built in Maestro [47] and then energy-minimized with MacroModel [48] applying the OPLS3e force field [49] to an energy gradient of 0.01 kcal/(mol Å). Docking simulations were performed with Glide in Standard Precision mode [50]. In case of compounds **5–11**, only poses superimposable to that **1** were retained for visual inspection and analysis, while for **14–20** only poses similar to that of compound **2** were considered.

5.3. Pharmacology

5.3.1. ELISA assays and IC₅₀ determination on EphA2-ephrin-A1 binding

ELISA assays were performed as previously described [30]. Briefly, 96-well ELISA high binding plates (Costar #2592) were coated with 100 μL /well of 1 $\mu\text{g mL}^{-1}$ (EphA2-Fc (R&D, Minneapolis, MN, USA 639-A2) and incubated overnight at 4 °C. The wells were washed 3 times with washing buffer solution and blocked for 1 h at 37 °C with a solution containing PBS +0.5% BSA. Afterwards,

the wells were washed again, and compounds were added at proper concentrations in 1% DMSO and incubated at 37 °C for 1 h. Then, biotinylated ephrin-A1-Fc (R&D Systems, BT602) was added at its K_D value for displacement studies or in a range from 1 to 2000 ng mL⁻¹ for saturation studies. Binding of biotinylated ephrin-A1-Fc to EphA2 was detected after 4 h through a standard Streptavidin-HRP-tetramethylbenzidine reaction and read in an ELISA plate reader (Sunrise, TECAN, Switzerland) at 450 nm. IC₅₀ and Ki values were determined using one-site competition non-linear regression analysis with Prism software (GraphPad Software Inc.). The selectivity of compound **14** was measured by coating the plate with all the EphA (R&D Systems, #SMPK1) and EphB (R&D Systems, #SMPK2) receptors and biotinylated ephrin-A1-Fc or biotinylated ephrin-B1-Fc (R&D Systems, #BT473) were used to study the binding on EphAs or EphBs, respectively, as described above.

5.3.2. Cell cultures

HUVE cells (Life Technologies, Waltham, MA, USA, CC035C) were grown in MEM 200 (Gibco, Thermo Fisher Scientific, Waltham, MA, USA, 097144) supplemented with LSGS kit (Gibco, Thermo Fisher Scientific, S003K), 1% penicillin–streptomycin solution (Euroclone, Milan, Italy, ECM0010D) and 10% fetal bovine serum (FBS, Euroclone, Milan, Italy, ECS0170L). PC3 human prostate adenocarcinoma cells (ECACC, Port Down, UK) were cultivated in Ham-F12 (Carlo Erba, Italy FA30WL0136500), supplemented with 7% FBS and 1% penicillin–streptomycin solution. Both cells were maintained in a humidified atmosphere of 95% air, 5% CO₂ at 37 °C.

5.3.3. Phosphorylation of EphA2 and cell lysates

PC3 cells were seeded onto 12-well plates at concentration of 10⁵ cells/well. Cells were pre-treated for 20 min with 0.3% DMSO, or titled compounds, and stimulated for 20 min with 0.25 μg mL⁻¹ ephrin-A1-Fc in serum free medium. Then, cells were rinsed with cold PBS and solubilized in lysis buffer. The lysates were transferred in micro-tubes, held for 15 min at 4 °C and centrifuged at 2000g for 5 min. BCA protein assay kit (Thermo Fisher Scientific, #23250) was used to measure the protein content of supernatant, which was standardized to 150 μg mL⁻¹. DuoSet IC Sandwich ELISA (R&D Systems, DYC4056 and DYC1095) was used as described in the manufacturer's protocol to measure EphA2 phosphorylation in cell lysates. 96-wells ELISA high binding plate (Costar, Corning, NY, USA, #9018) was coated with capture antibody at concentration of 4 μg mL⁻¹ and incubated overnight at room temperature. Then, wells were rinsed 5 times with washing solution and blocked with block buffer (PBS + 1% BSA) before the sample addition. After 1 h, 100 μL/well of standardized lysates were added and incubated for 2 h, lysates were then removed, and each well was filled with 100 μL of detection antibody (phospho-tyrosine HRP-conjugated antibody) and incubated for a couple of hours. Then, the detection antibody was aspired, wells were washed and the EphA2 phosphorylation levels were measured through a colorimetric reaction by adding Tetra-methylbenzidine solution as aforementioned.

5.3.4. In vitro angiogenesis

3*10⁴ HUVE cells were seeded in a BD Matrigel (BD Biosciences Bedford, MA, USA, #354230) pre-coated 96-wells plate. Cells were treated for 16 h with the compound **14** or with 0.3% DMSO and after that they were fixed with 3.7% formaldehyde (ROMIL, Waterbeach, Cambridge, UK, A9350) for 15 min at room temperature. Photographs of each well were taken by a digital camera mounted on a microscope (Eurotek, Orma, Italy, INV100TFL) to count the number of polygons. The results were expressed as the ratio between the number of polygons formed by the cells treated with the compound

and the untreated cells.

5.3.5. Chick-embryo chorioallantoic membrane (CAM) assay

Alginate plugs containing VEGF (4.5 pmol/embryo) (R&D Systems, 293-VE) with or without Compound **14** were placed on the CAM of fertilized white Leghorn chicken eggs at day 11. After 3 days, microvessels converging toward the implant were counted.

Declaration of competing interest

The authors declare that they have no known competing financial interests or personal relationships that could have appeared to influence the work reported in this paper.

Acknowledgments

This work was supported by Ministero dell'Università e della Ricerca, "Futuro in Ricerca" program(project code: RBFR10FXCP) to AL and Associazione Italiana Ricerca sul Cancro, Italy (AIRC IG 15211) to MT. This research benefits from the HPC (High Performance Computing) facility of the University of Parma, Italy - <http://www.hpc.unipr.it>.

Appendix A. Supplementary data

Supplementary data to this article can be found online at <https://doi.org/10.1016/j.ejmech.2020.112083>.

References

- [1] J.P. Himanen, N. Saha, D.B. Nikolov, Cell-cell signaling via Eph receptors and ephrins, *Curr. Opin. Cell Biol.* 19 (2007) 534–542.
- [2] E.B. Pasquale, Eph-ephrin bidirectional signaling in physiology and disease, *Cell* 133 (2008) 38–52.
- [3] E.B. Pasquale, Eph receptors and ephrins in cancer: bidirectional signalling and beyond, *Nat. Rev. Canc.* 10 (2010) 165–180.
- [4] B.W. Day, B.W. Stringer, A.W. Boyd, Eph receptors as therapeutic targets in glioblastoma, *Br. J. Canc.* 111 (2014) 1255–1261.
- [5] J. Wykosky, W. Debinski, The EphA2 receptor and ephrin-A1 ligand in solid tumors: function and therapeutic targeting, *Mol. Canc. Res.* 6 (2008) 1795–1806.
- [6] E. Binda, A. Visioli, F. Giani, G. Lamorte, M. Copetti, K.L. Pitter, J.T. Huse, L. Cajola, N. Zanetti, F. Di Meco, L. De Filippis, A. Mangiola, G. Maira, C. Anile, P. De Bonis, B.A. Reynolds, E.B. Pasquale, A.L. Vescovi, The EphA2 receptor drives self-renewal and tumorigenicity in stem-like tumor-propagating cells from human glioblastomas, *Canc. Cell* 22 (2012) 765–780.
- [7] K. Ogawa, R. Pasqualini, R.A. Lindberg, R. Kain, A.L. Freeman, E.B. Pasquale, The ephrin-A1 ligand and its receptor, EphA2, are expressed during tumor neovascularization, *Oncogene* 19 (2000) 6043–6052.
- [8] A.W. Boyd, P.F. Bartlett, M. Lackmann, Therapeutic targeting of EPH receptors and their ligands, *Nat. Rev. Drug Discov.* 13 (2014) 39–62.
- [9] N.V. Margaryan, L. Strizzi, D.E. Abbott, E.A. Seftor, M.S. Rao, M.J. Hendrix, A.R. Hess, EphA2 as a promoter of melanoma tumorigenicity, *Canc. Biol. Ther.* 8 (2009) 279–288.
- [10] G. Martiny-Baron, P. Holzer, E. Billy, C. Schnell, J. Brueggen, M. Ferretti, N. Schmiedeberg, J.M. Wood, P. Furet, P. Imbach, The small molecule specific EphB4 kinase inhibitor NVP-BHG712 inhibits VEGF driven angiogenesis, *Angiogenesis* 13 (2010) 259–267.
- [11] M. Tandon, S.V. Vemula, S.K. Mittal, Emerging strategies for EphA2 receptor targeting for cancer therapeutics, *Expert Opin. Ther. Targets* 15 (2011) 31–51.
- [12] A. Unzue, K. Lafleur, H. Zhao, T. Zhou, J. Dong, P. Kolb, J. Liebl, S. Zahler, A. Cafilisch, C. Nevado, Three stories on Eph kinase inhibitors: from in silico discovery to in vivo validation, *Eur. J. Med. Chem.* 112 (2016) 347–366.
- [13] G.L. Gravina, A. Mancini, A. Colapietro, S. Delle Monache, R. Sferra, F. Vitale, L. Cristiano, S. Martellucci, F. Marampon, V. Mattei, F. Beirinckx, P. Pujuguet, L. Saniere, G. Lorenzon, E. van der Aar, C. Festuccia, The small molecule ephrin receptor inhibitor, GLPG1790, reduces renewal capabilities of cancer stem cells, showing anti-tumour efficacy on preclinical glioblastoma models, *Cancers* 11 (2019) E359.
- [14] F.A. Mercurio, M. Leone, The sam domain of EphA2 receptor and its relevance to cancer: a novel challenge for drug discovery? *Curr. Med. Chem.* 23 (2016) 4718–4734.
- [15] X. Shi, V. Hapiak, J. Zheng, J. Muller-Greven, D. Bowman, R. Lingerak, M. Buck, B.C. Wang, A.W. Smith, A role of the SAM domain in EphA2 receptor activation, *Sci. Rep.* 7 (2017) 45084.

- [16] F.A. Mercurio, C. Di Natale, L. Pirone, D. Marasco, E. Calce, M. Vincenzi, E.M. Pedone, S. De Luca, M. Leone, Design and analysis of EphA2-SAM peptide ligands: a multi-disciplinary screening approach, *Bioorg. Chem.* 84 (2019) 434–443.
- [17] A. Petty, N. Idipilly, V. Bobba, W.J. Geldenhuys, B. Zhong, B. Su, B. Wang, Design and synthesis of small molecule agonists of EphA2 receptor, *Eur. J. Med. Chem.* 143 (2018) 1261–1276.
- [18] A. Petty, E. Myshkin, H. Qin, H. Guo, H. Miao, G.P. Tochtrop, J.T. Hsieh, P. Page, L. Liu, D.J. Lindner, C. Acharya, A.D. MacKerell Jr., E. Ficker, J. Song, B. Wang, A small molecule agonist of EphA2 receptor tyrosine kinase inhibits tumor cell migration in vitro and prostate cancer metastasis in vivo, *PLoS One* 7 (2012), e42120.
- [19] S.J. Riedl, E.B. Pasquale, Targeting the Eph system with peptides and peptide conjugates, *Curr. Drug Targets* 16 (2015) 1031–1047.
- [20] U. Lamminmaki, D. Nikolov, J. Himanen, Eph receptors as drug targets: single-chain antibodies and beyond, *Curr. Drug Targets* 16 (2015) 1021–1030.
- [21] Y. Choi, F. Syeda, J.R. Walker, P.J. Finerty Jr., D. Cuierrier, A. Wojciechowski, Q. Liu, S. Dhe-Paganon, N.S. Gray, Discovery and structural analysis of Eph receptor tyrosine kinase inhibitors, *Bioorg. Med. Chem. Lett.* 19 (2009) 4467–4470.
- [22] H.T. Zhao, J. Dong, K. Lafleur, C. Nevado, A. Cafilisch, Discovery of a novel chemotype of tyrosine kinase inhibitors by fragment-based docking and molecular dynamics, *ACS Med. Chem. Lett.* 3 (2012) 834–838.
- [23] P. Kolb, C.B. Kipouros, D.Z. Huang, A. Cafilisch, Structure-based tailoring of compound libraries for high-throughput screening: discovery of novel EphB4 kinase inhibitors, *Proteins* 73 (2008) 11–18.
- [24] A. Unzue, J. Dong, K. Lafleur, H.T. Zhao, E. Frugier, A. Cafilisch, C. Nevado, Pyrrolo[3,2-b]quinoxaline derivatives as types I-1/2 and II Eph tyrosine kinase inhibitors: structure-based design, synthesis, and in vivo validation, *J. Med. Chem.* 57 (2014) 6834–6844.
- [25] F.A. Mercurio, C. Di Natale, L. Pirone, D. Marasco, E. Calce, M. Vincenzi, E.M. Pedone, S. De Luca, M. Leone, Design and analysis of EphA2-SAM peptide ligands: a multi-disciplinary screening approach, *Bioorg. Chem.* 84 (2019) 434–443.
- [26] L. Gambini, A.F. Salem, P. Udompholkul, X.F. Tan, C. Baggio, N. Shah, A. Aronson, J. Song, M. Pellicchia, Structure-based design of novel EphA2 agonistic agents with nanomolar affinity in vitro and in cell, *ACS Chem. Biol.* 13 (2018) 2633–2644.
- [27] A. Lodola, C. Giorgio, M. Incerti, I. Zanotti, M. Tognolini, Targeting eph/ephrin interaction in cancer therapy, *Eur. J. Med. Chem.* 142 (2017) 152–162.
- [28] (a) M. Tognolini, I. Hassan-Mohamed, C. Giorgio, I. Zanotti, A. Lodola, Therapeutic perspectives of eph-ephrin system modulation, *Drug Discov. Today* 19 (2014) 661–669;
(b) A. Barquilla, E.B. Pasquale, Eph receptors and ephrins: therapeutic opportunities, *Annu. Rev. Pharmacol. Toxicol.* 55 (2015) 465–487;
(c) N. Saha, D. Robev, E.O. Mason, J.P. Himanen, D.B. Nikolov, Therapeutic potential of targeting the Eph/ephrin signaling complex, *Int. J. Biochem. Cell Biol.* 105 (2018) 123–133.
- [29] C. Festuccia, G.L. Gravina, C. Giorgio, A. Mancini, C. Pellegrini, A. Colapietro, S. Delle Monache, M.G. Maturro, R. Sferra, P. Chiodelli, M. Rusnati, A. Cantoni, R. Castelli, F. Vacondio, A. Lodola, M. Tognolini, UniPR1331, a small molecule targeting Eph/ephrin interaction, prolongs survival in glioblastoma and potentiates the effect of antiangiogenic therapy in mice, *Oncotarget* 9 (2018) 24347–24363.
- [30] M. Tognolini, M. Incerti, I. Hassan-Mohamed, C. Giorgio, S. Russo, R. Bruni, B. Lelli, L. Bracci, R. Noberini, E.B. Pasquale, E. Barocelli, P. Vicini, M. Mor, A. Lodola, Structure-activity relationships and mechanism of action of eph-ephrin antagonists: interaction of cholanic acid with the EphA2 receptor, *ChemMedChem* 7 (2012) 1071–1083.
- [31] M. Hatzia Apostolou, C. Polytarchou, Eph/ephrin system: in the Quest of Novel Anti-Angiogenic Therapies: commentary on Hassan-Mohamed et al., *Br J Pharmacol* 171: 5195–5208, *Br. J. Pharmacol.* 172 (2015) 4597–4599.
- [32] I. Hassan-Mohamed, C. Giorgio, M. Incerti, S. Russo, D. Pala, E.B. Pasquale, P. Vicini, E. Barocelli, S. Rivara, M. Mor, A. Lodola, M. Tognolini, UniPR129 is a competitive small molecule eph-ephrin antagonist blocking in vitro angiogenesis at low micromolar concentrations, *Br. J. Pharmacol.* 171 (2014) 5195–5208.
- [33] M. Tognolini, M. Incerti, A. Lodola, Are we using the right pharmacological tools to target EphA4? *ACS Chem. Neurosci.* 5 (2014) 1146–1147.
- [34] C. Giorgio, M. Incerti, M. Corrado, M. Rusnati, P. Chiodelli, S. Russo, D. Callegari, F. Ferlenghi, V. Ballabeni, E. Barocelli, A. Lodola, M. Tognolini, Pharmacological evaluation of new bioavailable small molecules targeting Eph/ephrin interaction, *Biochem. Pharmacol.* 147 (2018) 21–29.
- [35] S. Russo, D. Callegari, M. Incerti, D. Pala, C. Giorgio, J. Brunetti, L. Bracci, P. Vicini, E. Barocelli, L. Capoferri, S. Rivara, M. Tognolini, M. Mor, A. Lodola, Exploiting free-energy minima to design novel EphA2 protein-protein antagonists: from simulation to experiment and return, *Chemistry* 22 (2016) 8048–8052.
- [36] M. Incerti, S. Russo, D. Callegari, D. Pala, C. Giorgio, I. Zanotti, E. Barocelli, P. Vicini, F. Vacondio, S. Rivara, R. Castelli, M. Tognolini, A. Lodola, Metadynamics for perspective drug design: computationally driven synthesis of new protein-protein interaction inhibitors targeting the EphA2 receptor, *J. Med. Chem.* 60 (2017) 787–796.
- [37] J.P. Himanen, Y. Goldgur, H. Miao, E. Myshkin, H. Guo, M. Buck, M. Nguyen, K.R. Rajashankar, B. Wang, D.B. Nikolov, Ligand recognition by A-class Eph receptors: crystal structures of the EphA2 ligand-binding domain and the EphA2/ephrin-A1 complex, *EMBO Rep.* 10 (2009) 722–728.
- [38] S. Mitra, S. Duggineni, M. Koolpe, X. Zhu, Z. Huang, E.B. Pasquale, Structure-activity relationship analysis of peptides targeting the EphA2 receptor, *Biochemistry* 49 (2010) 6687–6695.
- [39] J.E. Saik, D.J. Gould, A.H. Keswani, M.E. Dickinson, J.L. West, Biomimetic hydrogels with immobilized ephrinA1 for therapeutic angiogenesis, *Bio-macromolecules* 12 (2011) 2715–2722.
- [40] D.K. Skovseth, A.M. Kuchler, G. Haraldsen, The HUVEC/Matrigel assay: an in vivo assay of human angiogenesis suitable for drug validation, *Methods Mol. Biol.* 360 (2007) 253–268.
- [41] D. Ribatti, B. Nico, A. Vacca, M. Presta, The gelatin sponge-chorioallantoic membrane assay, *Nat. Protoc.* 1 (2006) 85–91.
- [42] S. Sawamiphak, S. Seidel, C.L. Essmann, G.A. Wilkinson, M.E. Pitulescu, T. Acker, A. Acker-Palmer, Ephrin-B2 regulates VEGFR2 function in developmental and tumour angiogenesis, *Nature* 465 (2010) 487–491.
- [43] D.M. Brantley-Sieders, W.B. Fang, Y. Hwang, D. Hicks, J. Chen, Ephrin-A1 facilitates mammary tumor metastasis through an angiogenesis-dependent mechanism mediated by EphA receptor and vascular endothelial growth factor in mice, *Cancer Res.* 66 (2006) 10315–10324.
- [44] D. Pala, R. Castelli, M. Incerti, S. Russo, M. Tognolini, C. Giorgio, I. Hassan-Mohamed, I. Zanotti, F. Vacondio, S. Rivara, M. Mor, A. Lodola, Combining ligand- and structure-based approaches for the discovery of new inhibitors of the EphA2-ephrin-A1 interaction, *J. Chem. Inf. Model.* 54 (2014) 2621–2626.
- [45] R. Castelli, M. Tognolini, F. Vacondio, M. Incerti, D. Pala, D. Callegari, S. Bertoni, C. Giorgio, I. Hassan-Mohamed, I. Zanotti, A. Bugatti, M. Rusnati, C. Festuccia, S. Rivara, E. Barocelli, M. Mor, A. Lodola, Δ^5 -Cholenoyl-amino acids as selective and orally available antagonists of the eph-ephrin system, *Eur. J. Med. Chem.* 103 (2015) 312–324.
- [46] Schrödinger Glide, LLC, 2019. New York, NY.
- [47] Schrödinger Maestro, LLC, 2019. New York, NY.
- [48] MacroModel, Schrödinger, LLC, 2019. New York, NY.
- [49] Schrödinger, LLC, 2019. New York, NY.
- [50] R.A. Friesner, J.L. Banks, R.B. Murphy, T.A. Halgren, J.J. Klicic, D.T. Mainz, M.P. Repasky, E.H. Knoll, D.E. Shaw, M. Shelley, J.K. Perry, P. Francis, P.S. Shenkin, Glide: a new approach for rapid, accurate docking and scoring. 1. Method and assessment of docking accuracy, *J. Med. Chem.* 47 (2004) 1739–1749.